10. OPTICAL COHERENCE TOMOGRAPHY

- Optical coherence tomography (OCT) is a label-free (intrinsic contrast) technique that enables 3D imaging of tissues. The principle of its operation relies on *low-coherence interferometry*, i.e. interferometry with broadband light.

10.1. Low-coherence Interferometry (LCI).

- Consider a Michelson interferometer, where a broadband source is used for illumination (Fig. 1). Such sources include light emitting diodes (LEDs) superluminescent diodes (SLD), Ti:Saph lasers, and white light lamps.

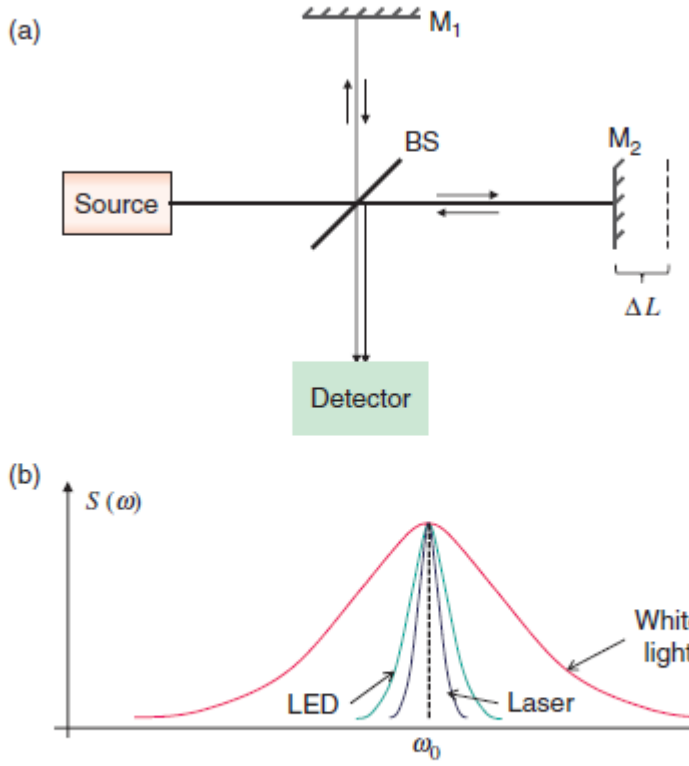

FIGURE 7.1 (*a*) LCI using a Michelson interferometer. Mirror M2 adjusts the path-length delay between the two arms. (*b*) Illustration of optical spectrum for various sources.

Figure 10-1. LCI using a Michelson interferometer. Mirror M_2 adjust the path-length delay between the two arms.

- A qualitative comparison between the optical spectrum of a broadband source and that of a laser is shown in Fig. 2.
- We found previously that the *coherence time* is of the order of $\tau_c \simeq \frac{\lambda_0^{\,2}}{\Delta\lambda}$, where λ_0 is the central wavelength and λ the bandwidth.

- The total instantaneous field at the detector is the sum of the two fields.

$$U(t) = U_1(t) + U(t+\tau) \qquad (10.1)$$

- τ is the delay introduced by the mobile mirror (M_2).
- The intensity at the detector is the modulus-squared average of the field,

$$\begin{aligned} I(\tau) &= \left\langle \left| U(t) \right|^2 \right\rangle \\ &= I_1 + I_2 + \left\langle U_1(t) \cdot U_2^{*}(t+\tau) \right\rangle + \left\langle U_1^{*}(t) \cdot U_2(t+\tau) \right\rangle \qquad (10.2) \\ &= I_1 + I_2 + 2\,\mathrm{Re}\left[\Gamma_{12}(\tau) \right], \end{aligned}$$

- Angular brackets denote temporal averaging.
- In Eq. 2 we recognize the temporal cross-correlation function Γ_{12}, defined as

$$\begin{aligned} \Gamma_{12}(\tau) &= \left\langle U_1(t) \cdot U_2^{*}(t+\tau) \right\rangle \\ &= \int U_1(t) \cdot U_2^{*}(t+\tau)\, dt \end{aligned} \qquad (10.3)$$

- From Eq. 3, we see that the cross-correlation function can be measured experimentally by simply scanning the position of M_2. Using the Wiener-Kintchin theorem, Γ_{12} can be expressed as a Fourier transform

$$\Gamma_{12}(\tau) = \int W_{12}(\omega) \cdot e^{-i\omega\tau} d\omega. \qquad (10.4)$$

- W_{12} is known as cross-spectral density, defined as

$$W_{12}(\omega) = U_1(\omega) \cdot U_2^{*}(\omega) \qquad (10.5)$$

- We assume that the fields on the two arms are identical.
- Thus, if $U_1(\omega) = U_2(\omega)$ reduces to the spectrum of light, S, and Γ_{12} reduces to the autocorrelation function, Γ,

$$\Gamma(\tau) = \int S(\omega) \cdot e^{-i\omega\tau} d\omega \qquad (10.6)$$

- The intensity measured by the detector has the form shown in Fig. 3a.

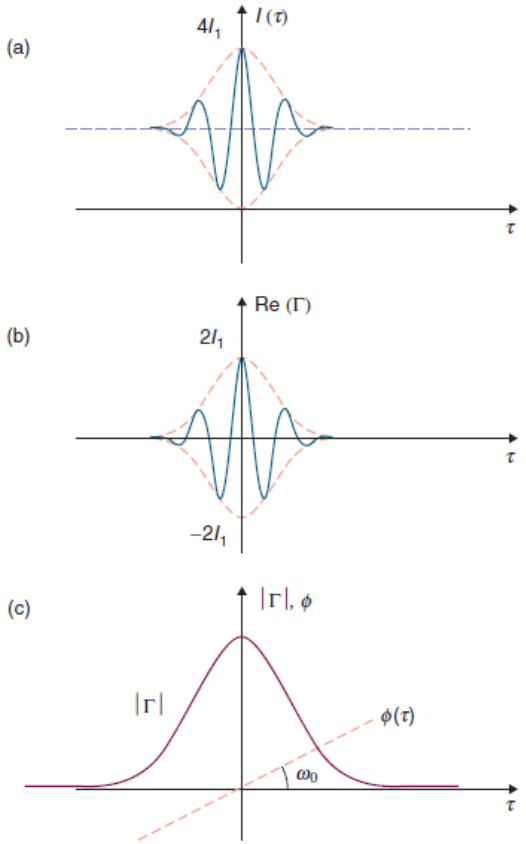

FIGURE 7.2 Low coherence interferometry with a perfectly balanced interferometer.

- Subtracting the signal at large τ (the Δc component), which equals $2I_1$ for perfectly balanced interferometers, the real part of Γ is obtained as shown in Fig. 3b.

- Using a Hilbert transform, the imaginary part of Γ can be obtained,

$$\mathrm{Im}\left[\Gamma(\tau)\right] = -\frac{1}{\pi} P \int \frac{\mathrm{Re}\left[\Gamma(\tau')\right]}{\tau - \tau'} d\tau', \qquad (10.7)$$

- P indicates a principal value integral.
- The complex analytic signal associated with $\mathrm{Re}\left[\Gamma(\tau)\right]$ is the (complex) function Γ, characterized by an amplitude and phase (Fig. 3c).

- For a symmetric spectrum centered at ω_0, $S(\omega) = S'(\omega - \omega_0)$, it can be easily shown (via the shift theorem) that the autocorrelation function has the form

$$\begin{aligned}\Gamma(\tau) &= \int S'(\omega - \omega_0) \cdot e^{-i\omega\tau} d\omega \\ &= e^{i\omega_0\tau} \int S'(\omega) \cdot e^{-i\omega\tau} d\omega \\ &= \left|\Gamma(\tau)\right| \cdot e^{i\omega_0\tau}\end{aligned} \qquad (10.8)$$

- Equation 8 establishes that the envelope of Γ equals the Fourier transform of the spectrum. Since we assumed a symmetric spectrum, the envelope is a real function. Further, the phase (modulation) of Γ is linear with τ, where the shape is given by the mean frequency, $\phi(\tau) = \omega_0\tau$.

10.2. Effects of unbalanced dispersion.

- The fields on the two arms of the interferometer are rarely identical. While the amplitude of the two fields can be easily matched via attenuators, making the optical pattern identical is more difficult.
- Here, we will study the effect of dispersion due to the beams passing through different lengths of dispersion media, such as glass. This is always the case when using a thick beam splitter in the Michelson interferometer (Fig. 4). Typically, the beam splitter is made of a piece of glass half-silvered on one side.

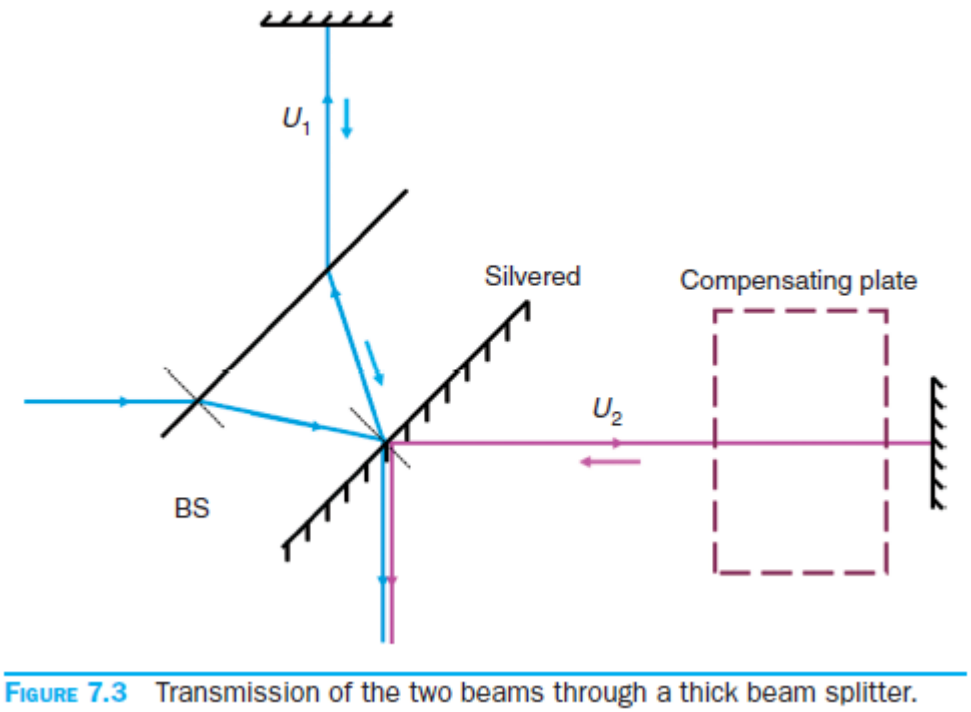

FIGURE 7.3 Transmission of the two beams through a thick beam splitter.

Figure 10-4. Transmission of the two beams through a thick beam splitter.

- It can be seen in Fig. 4 that field U_1 passes through the glass 3 times, while field U_2 passes through only once. Therefore the phase difference between U_1 and U_2 has the frequency dependence

$$\phi(\omega) = 2k(\omega) \cdot L \qquad (10.9)$$

- where L is the thickness of the beam splitter.
- This spectral phase can be expanded in Taylor series around the central frequency,

$$\phi(\omega) = \phi(\omega_0) + 2L \left.\frac{dk(\omega)}{d\omega}\right|_{\omega=\omega_0} (\omega - \omega_0) + L \cdot \left.\frac{d^2k}{d\omega^2}\right|_{\omega=\omega_0} (\omega - \omega_0)^2 + \ldots \quad (10.10)$$

- In Eq. 10, we define the following quantities:
- Phase shift of mean frequency:

$$\phi(\omega_0) = \frac{2\omega_0}{c} \cdot L, \quad (10.11)$$

- Group velocity:

$$v_g = \left.\frac{d\omega}{dk}\right|_{\omega=\omega_0}, \quad (10.12)$$

- Group velocity dispersion (GVD)

$$\beta_2 = \frac{d^2 k}{d\omega^2} = \frac{\partial}{\partial \omega}\left(\frac{1}{v_g}\right) \qquad (10.13)$$

- GVD has units of $s^2/m = s/Hz \cdot m$ and defines how a phase spreads in the material due to dispersion effects. GVD is sometimes defined as a derivative with respect to wavelength.
- We can now express the cross-spectral density as

$$\begin{aligned} W_{12}(\omega) &= U_1(\omega) \cdot U_1^*(\omega) \cdot e^{i\phi(\omega)} \\ &= S(\omega) \cdot e^{i\phi(\omega)} \qquad (10.14) \\ &= S'(\omega - \omega_0) \cdot e^{i\phi(\omega_0)} \cdot e^{i\frac{2L}{v_g}(\omega-\omega_0)} \cdot e^{iL\beta_2(\omega-\omega_0)^2} \end{aligned}$$

- In Eq. 14 we assumed that the two fields are of equal amplitude, and differ only through the phase shift due to the unbalanced dispersion. The temporal cross-correlation function is obtained by taking the Fourier transform of Eq. 14.
- Consider first the case of negligible GVD, $\beta_2 = 0$:

$$\begin{aligned}\Gamma_{12}(\tau) &= e^{i\phi(\omega_0)} \int S'(\omega-\omega_0)\cdot e^{i\frac{2L}{v_g}(\omega-\omega_0)} \cdot e^{-i\omega\tau} d\omega \\ &= e^{i\omega_0\tau} \cdot e^{i\phi(\omega_0)} \int S'(\omega-\omega_0)\cdot e^{-i(\omega-\omega_0)\left(\tau-\frac{2L}{v_g}\right)} d(\omega-\omega_0)\end{aligned} \qquad (10.15)$$

- The integral in Eq. 15 amounts to the shifted autocorrelation envelope, such that Eq. 15 becomes

$$\Gamma_{12}(\tau) = \left|\Gamma\left(\tau-\frac{2L}{v_g}\right)\right| \cdot e^{i(\omega_0\tau+\phi(\omega))} \qquad (10.16)$$

- Equation 16 establishes that, in the absence of GVD, there is no shape change in either the amplitude or the phase of the original correlation function.

- The phase shift, $\phi(\omega_0)$, is due to the zeroth order (phase velocity) term in the expansion of Eq. 10, while the envelope shift, or *group delay*, is caused by the first (group velocity) term (Fig. 4).

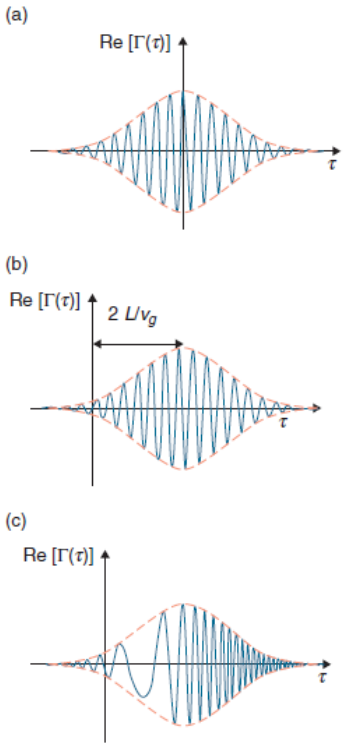

FIGURE 7.4
(*a*) Autocorrelation function for a perfectly balanced detector. (*b*) Group delay (first order) effects. (*c*) GVD (second order) effects.

- The envelope shift, $\tau_0 = 2L/v_g$, can be conveniently compensated by adjusting the mobile mirror of the interferometer. If the beam splitter material has no GVD, the interferometer operates as if it is perfectly balanced.
- Let us investigate separately the effect of the GVD itself. The cross-correlation has the form

$$\Gamma_{12}(\tau) = \int S'(\omega - \omega_0) \cdot e^{iL\beta_2(\omega-\omega_0)^2} \cdot e^{-i\omega\tau} d\omega. \quad (10.17)$$

- The Fourier transform in Eq. 17 yields a convolution between the Fourier transform of S' and that of $e^{iL\beta_2\omega^2}$, i.e.

$$\Gamma_{12}(\tau) = \Gamma(\tau) * e^{-i\frac{\tau^2}{4\beta_2 L}} / \sqrt{2\beta_2 L} \quad (10.18)$$

- Equation 18 establishes that the cross-correlation function Γ_{12} is broader than Γ due to the convolution operation. This effect is to ultimately degrade the axial resolution of OCT images.

- In practice, great effort is devoted towards compensating for unbalanced dispersion in the interferometer.

10.3. Optical coherence tomography.

- OCT is typically implemented in fiber optics, where one of the mirrors in the interferometer is replaced by a 3D specimen. Thus, the depth-information is provided by virtue of the LCI discussed above. In order to obtain x-y resolution, the sample arm must be equipped with a 2D scanning system, typically comprised of galvo-mirrors (Fig. 5).

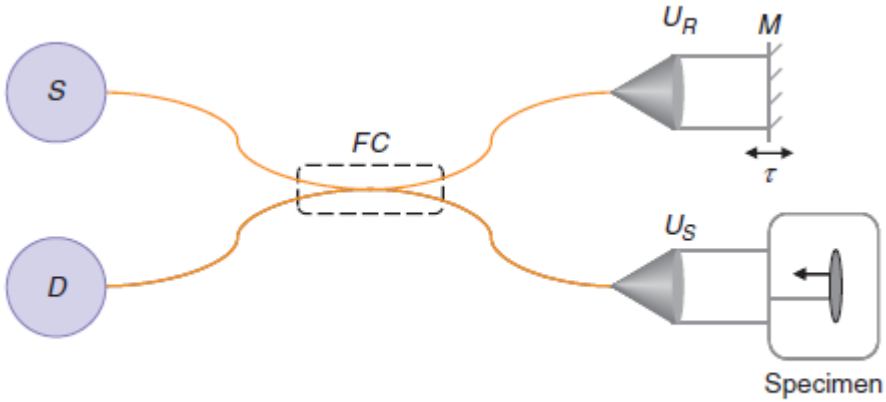

FIGURE 7.5 Fiber optics, time domain OCT.

- At each point (x, y), the OCT signal consists of the cross-correlation Γ_{12} between the reference field U_R and specimen field U_S, which can be expressed as the Fourier transform of the cross-correlation density

$$W_{12}(\omega) = U_S(\omega) \cdot U_R^*(\omega) = S(\omega) \cdot \tilde{h}(\omega), \qquad (10.19)$$

- $S(\omega) = U_R(\omega) \cdot U_R(\omega)$ is the spectrum of the source.
- In Eq. 19, we introduced the *spectral modifier* $\tilde{h}(\omega)$, which is a complex function characterizing the spectral response of the specimen,

$$U_S(\omega) = U_R(\omega) \cdot \tilde{h}(\omega). \qquad (10.20)$$

- The two fields are initially identical, i.e. the interferometer is balanced, and the specimen is modifying the incident field via $\tilde{h}(\omega)$.

- The resulting cross-correlation obtained by measurement is a convolution operation

$$\Gamma_{12}(\tau) = \Gamma(\tau) * h(\tau), \qquad (10.21)$$

- *h* is the time response function of the sample, the Fourier transform of $\tilde{h}(\omega)$,

$$h(\tau) = \int \tilde{h}(\omega) \cdot e^{-i\omega\tau} d\omega. \qquad (10.22)$$

10.3.1. Depth-resolution in OCT.

- The LCI configuration depicted in Fig. 1 is recovered by introducing a δ response function, $h(\tau)=\delta(\tau)$.
- In this case the cross-correlation reduces to

$$\Gamma_{12}(\tau)=\Gamma(\tau-\tau_0), \qquad (10.23)$$

- $\tau_0=\dfrac{z}{2c}$ is the time delay due to the depth location of the reflector (Fig. 6)

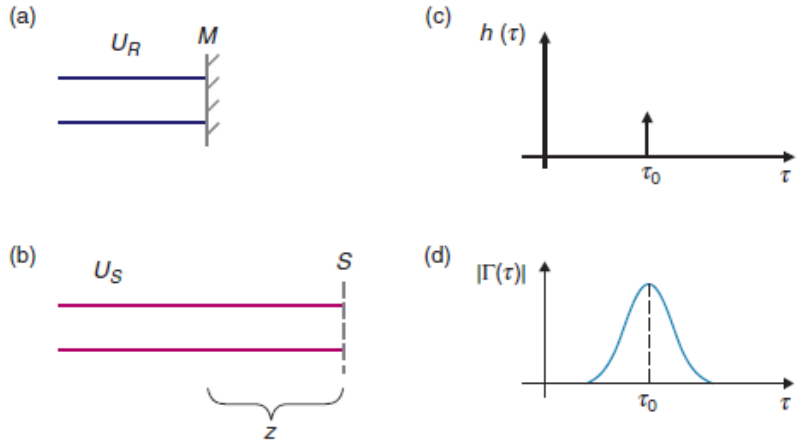

FIGURE 7.6 Response from a reflector at depth z: (*a*) the reference arm; (*b*) the sample arm; (*c*) the ideal response function from the mirror in (*b*); (*d*) the measured response from the mirror in (*b*).

- OCT images are obtained by retaining the modulus of Γ_{12}, which is a complex function $\Gamma_{12}(\tau) = \left|\Gamma_{12}(\tau)\right| \cdot e^{i\left[\omega_0 \tau + \phi(\tau)\right]}$.
- The high frequency component (carrier), $e^{i\omega_0 \tau}$, is filtered via demodulation (low-pass filtering). Equation 23 gives access to the impulse response function of OCT, $\left|\Gamma(\tau)\right|$.
- As in Fig. 6b the width of the envelope of Γ establishes the ultimate resolution in locating the reflector's position. This resolution in time is nothing more that the coherence time of the source, τ_C.
- In terms of depth, this resolution limit is the *coherence length*, $l_C = v\tau_C$, with v the speed of light in the medium. This result establishes the need for broadband sources in OCT, as $\tau_C \propto \frac{1}{\Delta\omega}$.

- The coherence length is the absolute best resolution that OCT can deliver. The performance can be drastically reduced by dispersion effects.
- The specimen itself can “unbalance” the interferometer. Consider a reflective surface buried in a medium characterized by dispersion (e.g. a tumor located at a certain depth in the tissue), as illustrated in Fig. 7.

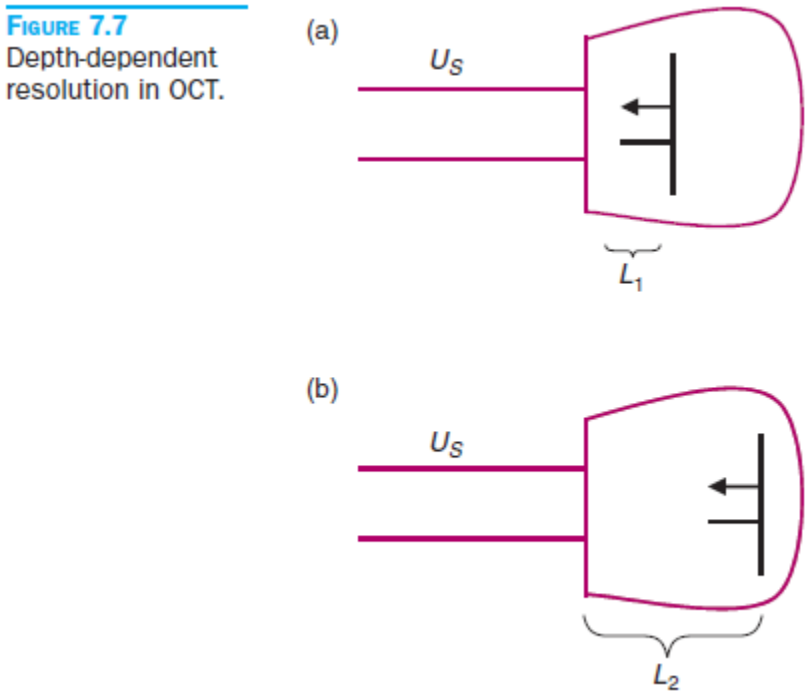

Figure 10-8. Depth-dependent resolution in OCT.

- Even when the attenuation due to depth propagation is negligible (weakly scattering medium), the spectral phase accumulate differs for the two depths (see Eq. 18),

$$\Gamma_{12}\left(\tau, L_{1,2}\right) = \Gamma\left(\tau\right) * e^{-i\frac{\tau^2}{4\beta_2 L_{1,2}}} \Big/ \sqrt{2\beta_2 L_{1,2}}, \qquad (10.24)$$

- β_2 is the GVD of the medium above the reflector.
- The signal is broader from the reflector that is placed deeper ($L_2 > L_1$) in the medium, i.e. the axial resolution degrades with depth.

10.3.2. Contrast in OCT.

- Contrast in OCT is given by differences in reflectivity between different structures. Contrast in a transverse (x-y, en face) OCT image depends on depth.

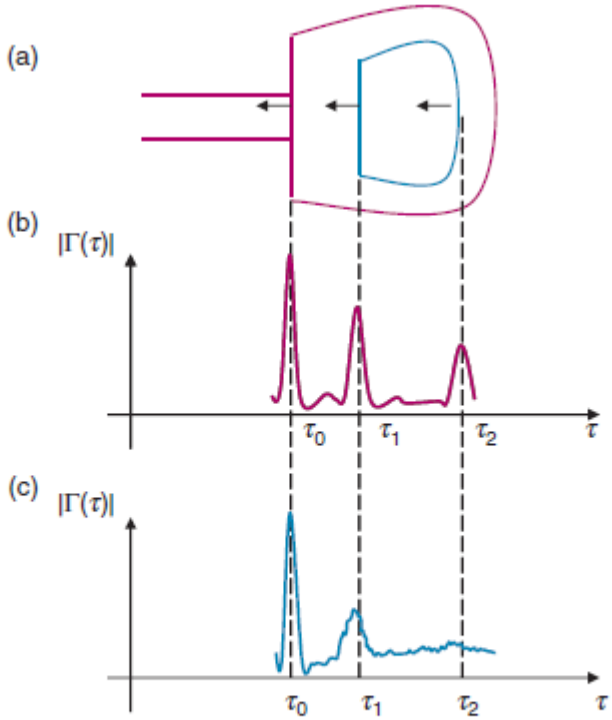

FIGURE 7.8 Signals from an object surrounded by scattering medium, illustrated in (*a*). (*b*) Depth-resolved signals for *weakly scattering* medium. (*c*) Depth-resolved signals for *strongly scattering* medium.

- Figure 8 illustrates the change in SNR with depth. The scattering properties of the surrounding medium is an important variable that affects depth-dependent SNR. Thus, the backscattering limits the contrast to noise ratio in an x-y image.

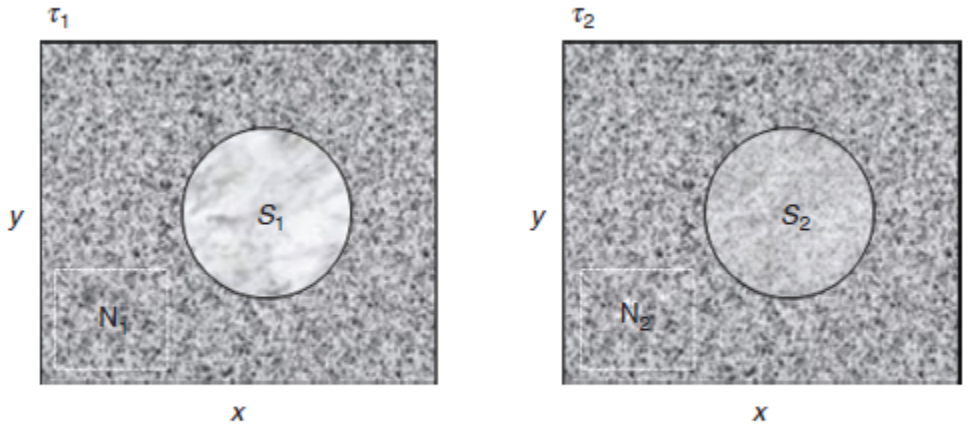

FIGURE 7.9 En-face images corresponding to the two time-delays shown in Fig. 7.8.

- The signal and noise must be defined locally, i.e. at each depth, for which the signal to noise has the form

$$SNR(\tau) = \frac{|\Gamma(\tau)|}{\sigma_N(\tau)}, \qquad (10.25)$$

- $\sigma_N(\tau)$ is the standard deviation of the noise around the time delay τ.
- This noise component is due to mechanical vibrations, source noise, detection/electronic noise, and most importantly, due to the scattering from the medium that surrounds the structure of interest.
- In an en face image, we can define the contrast to noise ratio as

$$CNR(\tau) = \frac{\left\| |\Gamma_A(\tau)| - |\Gamma_B(\tau)| \right\|}{\sigma_N(\tau)}, \qquad (10.26)$$

- where A and B are two structures of interest.